European Journal of Medicinal Chemistry 44 (2009) 2128–2134

Contents lists available at ScienceDirect

European Journal of Medicinal Chemistry

journal homepage: http://www.elsevier.com/locate/ejmech

Original article

Computational modeling and surface plasmon resonance analyses in the assessment of peptide ligands interacting with fibrin γ(312–324) epitope

Ilaria Massarelli [a], Anna M. Bianucci [b,*], Federica Chiellini [a], Chaim Eidelman [c], Emo Chiellini [a]

[a] BIOlab, UdR INSTM, Department of Chemistry and Industrial Chemistry, University of Pisa, Via Vecchia Livornese 1291, 56122 San Piero a Grado, Pisa, Italy
[b] Department of Pharmaceutical Science, Via Bonanno 6, 56123 Pisa, Italy
[c] Novetide Limited, Deshanim Road, 26111 Haifa Bay, Israel

ARTICLE INFO

Article history:
Received 19 July 2007
Received in revised form
10 October 2008
Accepted 20 October 2008
Available online 5 November 2008

Keywords:
Fibrin
GBSA
SPR (surface plasmon resonance)

ABSTRACT

Fibrin represents a suitable target for addressing delivery systems loaded by fibrinolytic drugs. Selective ligands capable to recognize fibrin could be used as targeting moieties for such systems. In this study the interactions between the γ(312–324) epitope of human fibrin and peptidic ligands were analyzed by using experimental and computational methods. Binding free energies were calculated through the molecular mechanics/generalized born surface area approach. Good qualitative agreements between the experimental and calculated data were obtained. The binding affinity seems to be well correlated ($R^2 = 0.69$) with the changes of the nonpolar solvation energy term computed from solvent-accessible surface area calculation. These results indicate that current methods of estimating binding free energies are efficient for achieving information on protein–ligand interactions.

1. Introduction

Fibrin is a protein involved in the clotting of blood. It is a fibrillar protein that is polymerized to form a "mesh" that gives rise to a haemostatic plug or clot (in conjunction with platelets) over a wound site. Fibrin is made from its zymogen fibrinogen, a soluble plasma glycoprotein that is synthesized by the liver. Several processes, in the coagulation cascade, activate the zymogen prothrombin to the serine protease thrombin, which is responsible for converting fibrinogen into fibrin. Fibrin is then cross-linked by factor XIII to form a clot [1]. Some modifications that occur after fibrinogen/fibrin conversion regard the exposure of critical sequences that were buried in the fibrinogen molecule. In particular, several sequences have been discovered and identified as fibrin-specific epitopes [2]. Among them, according to our previous evaluations [3], we chose the γ(312–324) epitope [4] as starting point for the design of ligands characterized by high affinity and specificity for human fibrin. These ligands may be used as targeting moieties in therapeutic applications, such as driving systems for targeted delivery of fibrinolytic drugs, thus allowing avoidance of the unwanted severe side effects due to the systemic administration of these kinds of drugs. Surface plasmon resonance (SPR) is a biochemical technique for directly measuring protein–protein/ligand interactions [5]. The choice of the SPR experimental technique was made because neither endogenous nor synthetic high affinity ligands were known for this biological target before our study. That made the most current procedure for experimental validation, based on radio-ligand binding displacement, impossible to be accomplished.

In a previous work by us SPR measurements were carried out [3] in order to estimate the affinities between human fibrin with a set of representative peptidic ligands specifically designed upon molecular docking calculations. Here new trials were performed to overcome drawbacks related to the possible loss of native conformation of fibrin once immobilized on the sensor chip, by applying some minor changes to the protocol previously exploited.

The immobilization in the SPR experiments of the fibrin molecule on a sensor chip, in fact, may cause slight changes in the fibrin conformation thus affecting the interaction between the selected ligands and the binding site on the fibrin epitope, with substantial differences with respect to its physiological state.

Since the SPR experiments imply the risk that the assayed fibrin may not be exactly in its native conformation, due its binding with the sensor chip, the comparison between calculated and

Abbreviations: GBSA, generalized born surface area; SPR, surface plasmon resonance; MM, molecular mechanics; MD, molecular dynamics; SASA, solvent-accessible surface area.

* Corresponding author. Tel.: +39 0502219575; fax: +39 0502219605.
E-mail address: bianucci@dcci.unipi.it (A.M. Bianucci).

0223-5234/$ – see front matter © 2008 Elsevier Masson SAS. All rights reserved.
doi:10.1016/j.ejmech.2008.10.029

Table 1
Fibrin–peptide binding affinity data measured at flow rates of 5 and 30 μl/min, with their mean values and relative SEM.

Peptides	K_D (μM) (*F*: 5 μl/min)	K_D (μM) (*F*: 30 μl/min)	Mean K_D (μM)	SEM
H–LysGluLys–NH_2	35.0	15.0	25.0	10.0
H–LysGluArg–NH_2	13.0	21.9	17.5	4.5
H–LysAspArg–NH_2	52.6	16.2	34.4	18.2
Ac–ArgAspLys AspArg–OH	30.4	16.8	23.6	6.8
H–ArgAspLys AspArg–NH_2	0.3	0.2	0.25	0.05

experimental results, obtained by the SPR technique, is expected to supply useful information for further improvement of the design work aimed at obtaining optimal recognition molecules for fibrin itself. Molecular dynamics (MD) simulation supplies indeed an useful tool for investigating protein–ligand interactions at the atomic level. A new computational method, MM/GBSA (molecular mechanics/generalized born surface area) [6], was recently proposed for calculating the binding free energies of macromolecular arrays. The free energy of these systems consists of contributions from van der Waals and electrostatic energies, nonpolar and electrostatic solvation energies, and relative solute entropy effects [7]. The van der Waals and electrostatic energies are calculated by using molecular mechanics (MM); the nonpolar solvation energy is estimated using empirical methods based on the solvent-accessible surface area (SASA); and the electrostatic solvation energy is obtained by using a continuum solvation model. The entropy contribution can be estimated by using normal-mode analysis [8].

In the present work new SPR studies were performed and the MM/GBSA was used to estimate binding free energies for the complexes between a globular sub-domain containing the γ(312–324) epitope of fibrin [3] and the peptides designed as potential paratopes. By comparing experimental and calculated binding Δ*G*s a good correlation was observed; in particular factors dominating the binding affinity were identified.

2. Methods

2.1. Free energy calculations

The three-dimensional model of the globular domain of the γ chain of polymerized fibrin [including the γ(312–324) epitope] used as initial structure in the MD simulation was previously built up [3] by starting from an X-ray-determined structure (ID: 1FZC) available in the protein data bank (PDB) [9]. Furthermore, the structures of the five tested peptides were previously designed upon molecular docking optimization in the same 3D model [3].

The MM/GBSA technique was used to estimate the solvation and binding free energies of macromolecules and their complexes. Accordingly, the average total free energy of the system, *G*, is calculated as

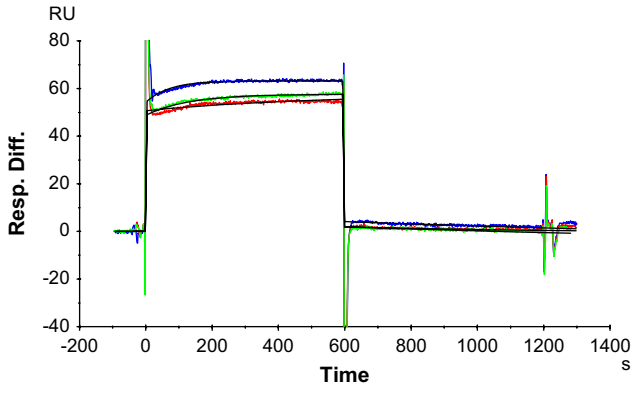

Fig. 1. Analysis of the binding of Ac–ArgAspLysAspArg–OH ligand to immobilized fibrin. In the example only three of the tested concentrations of the ligand (blue 1, green 0.5 and red 0.1 mM) were reported. The ligand was added to immobilized fibrin, and its association and dissociation were monitored in real time while recording the resonance signal (response). Both experimental and corresponding fitted curves are shown. (For interpretation of the references to colour in this figure legend, the reader is referred to the web version of this article.)

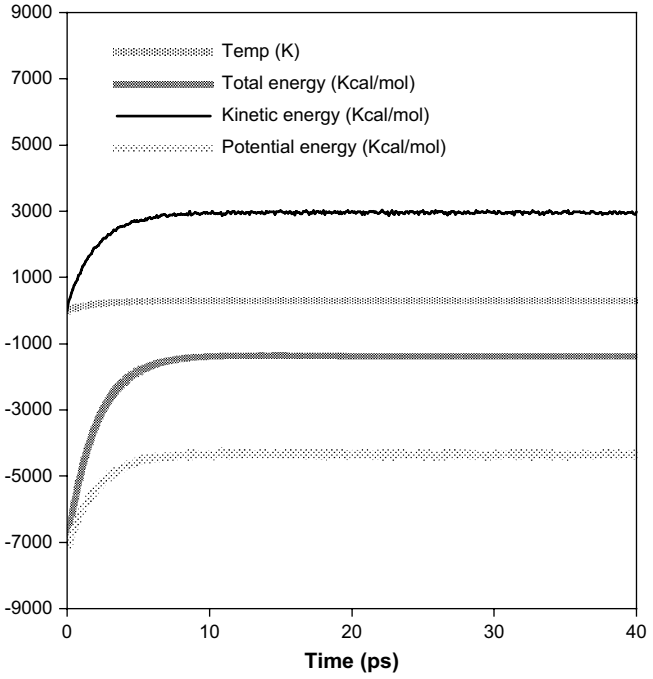

Fig. 2. MD simulations: changes of temperature, kinetic, potential and total energies during heating (0–5 ps), equilibration (5–20 ps) and collection phases (20–40 ps) of H–ArgAspLysAspArg–NH_2/fibrin complex.

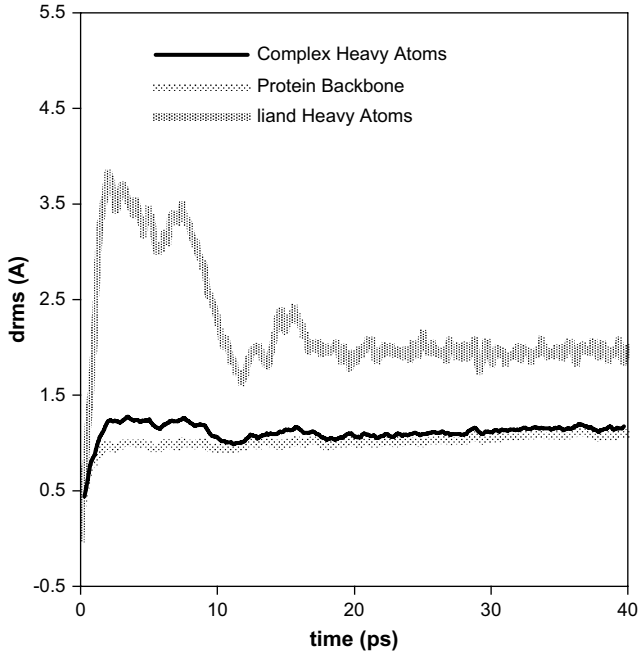

Fig. 3. Rms deviations for all heavy atoms, protein backbone main-chain atoms, and ligand heavy atoms from initial structures as a function of simulation time.

Table 2
Variation of contributes during the simulations.

Peptides	ΔE_{MM}[a]	$\Delta G_{nonpolar}$	ΔG_{polar}	ΔSASA	$T\Delta S$	ΔG_{calc}	ΔG_{exp}
H–LysGluLys–NH_2	−611.90	−2.88	542.24	−521.53	−72.45	−6.49	−6.28
H–LysGluArg–NH_2	−597.54	−3.36	544.15	−611.10	−59.46	−3.69	−6.49
H–LysAspArg–NH_2	−653.85	−1.66	586.05	−249.26	−95.28	19.42	−6.09
Ac–ArgAspLysAspArg–OH	−237.44	−2.48	158.86	−448.90	−121.07	33.60	−6.32
H–ArgAspLysAspArg–NH_2	−652.44	−4.26	539.33	−776.03	−93.59	−30.17	−8.99

[a] All energies are in Kcal/mol, ΔSASA in Å^2.

$$G = E_{MM} + G_{polar} + G_{nonpolar} - TS \quad (1)$$

where, a polar solvation energy term G_{polar} is computed in continuum solvent using a generalized born (GB) model and a nonpolar solvation energy term $G_{nonpolar}$ is computed from SASA calculations using Eq. (2) for each isolated state (receptor, ligand, or complex) [10].

$$G_{nonpolar} = (0.00542 * SASA) + 0.92 \quad (2)$$

The E_{MM} term in Eq. (1) is a sum of the electrostatic (Coulombic), van der Waals (Lennard–Jones), and internal energies (bonds, angles, and dihedrals).

Entropic effects may be included (TS term) where T is the temperature and the entropy S is typically estimated on the basis of commonly known statistical formulae and normal-mode analysis of representative snapshots of energy-minimized structures from a molecular dynamics (MD) trajectory. The binding free energy is then estimated from Eq. (3).

$$\Delta G_{bind} = G_{complex} - G_{protein} - G_{ligand}$$
$$= \Delta E_{MM} + \Delta G_{polar} + \Delta G_{nonpolar} - T\Delta S \quad (3)$$

The thermally averaged energy terms in Eq. (3) are obtained from MD sampling.

2.2. Generalized born molecular dynamics simulations (GB-MD)

A two-stage conjugant gradient energy minimization protocol was applied to each individual species (complex, receptor, or ligand) prior to the MD simulations. At first, energy minimization was performed for each species in which only the heavy atoms were restrained (to their crystallographic positions for the receptor and to their previously optimized positions for the ligands) using a harmonic potential of 1000.0 kcal/mol Å^2. A second restrained minimization was then performed using a much weaker force constant of 5.0 kcal/mol Å^2 in which only the main-chain atoms were restrained. Both minimizations employed a distance dependent dielectric constant ($4r$) and loose tolerance for convergence. After the minimizations, molecular dynamics simulations were started without explicit water using the pairwise GB continuum solvent model of Hawkins and co-workers [11,12] implemented in the SANDER module of AMBER7 [13]. No cutoff was employed during the GB-MD simulations.

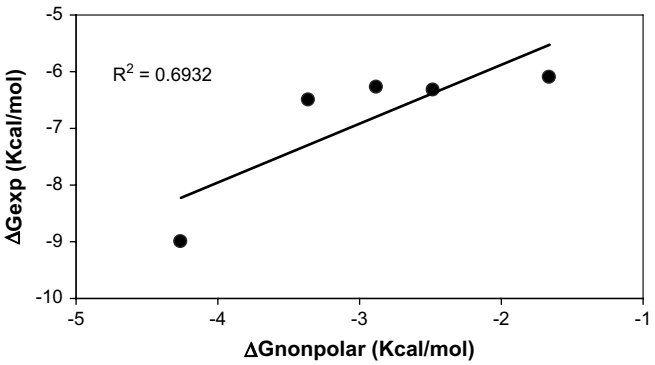

Fig. 4. Correlation between $\Delta G_{nonpolar}$ and experimental binding free energy.

Simulations employed 1 fs time step for 40,000 steps corresponding to a total of 40 ps of GB-MD. The final desired temperature of 298 K was obtained by requesting a heating cycle from 0 to 298 K over the course of the first 5000 MD steps with temperature regulation maintained via coupling to an external heat bath using the Berendsen scheme [14] and a coupling time constant of 1.0 ps. Main-chain atoms were lightly restrained using a weak harmonic force constant of 5.0 kcal/mol Å^2, and the SHAKE [15] algorithm was applied to constrain bonds involving hydrogen atoms. Average structural and energetic quantities exploited to estimate binding affinities between ligands and fibrin were computed using 200 snapshots from the last 20 ps of the MD trajectory. In particular the various energy terms in Eq. (1) were computed as follows. Electrostatic (Ecoul), van der Waals (Evdw), and internal energies were obtained using the SANDER module in AMBER7. Polar energies (G_{polar}) were obtained from the AMBER7 (GB energies) programs using dielectric constants of 1 and 80 to represent gas and water phases, respectively. Nonpolar energies ($G_{nonpolar}$) were determined from Eq. (2) using SASAs computed with the MOLSURF program [13].

Due to the huge amount of computer time required, solute entropies were computed by using five energy-minimized snapshots obtained by exploiting the NMODE module in AMBER7. It is worth to point out that the NMODE calculations constitute an N3 problem, where N is the number of atoms involved, so making the computational approach very demanding in terms of computational effort. To simplify the calculations, the residues within an 8-Å sphere around the ligand were cut out from an MD snapshot for each ligand–protein complex. The open valences were saturated by adding hydrogen atoms by the Insight program (Accelrys) [16].

To reduce the statistical error, a snapshot was extracted and analyzed every 5 ps. The final entropy calculation was averaged over five snapshots. Prior to the normal-mode calculations, each species (complex, receptor, or ligand) was subjected to a conjugant gradient energy minimization using a distance dependent dielectric ($4r$) and convergence tolerance drms of 1.0×10^{-4} kcal/mol Å. Subsequently, the structures were further minimized with the Newton–Raphson algorithm for 500 steps using the NMODE program until a convergence tolerance drms $= 1.0 \times 10^{-5}$ kcal/mol Å was reached [17].

Table 3
Correlation coefficient between components of calculated binding free energies and measured binding free energies.

	ΔG_{calc}	ΔG_{SA}	ΔSASA	ΔE_{MM}	ΔG_{GB}	$T\Delta S$
R^2	0.59	0.69	0.64	0.09	0.03	0.005

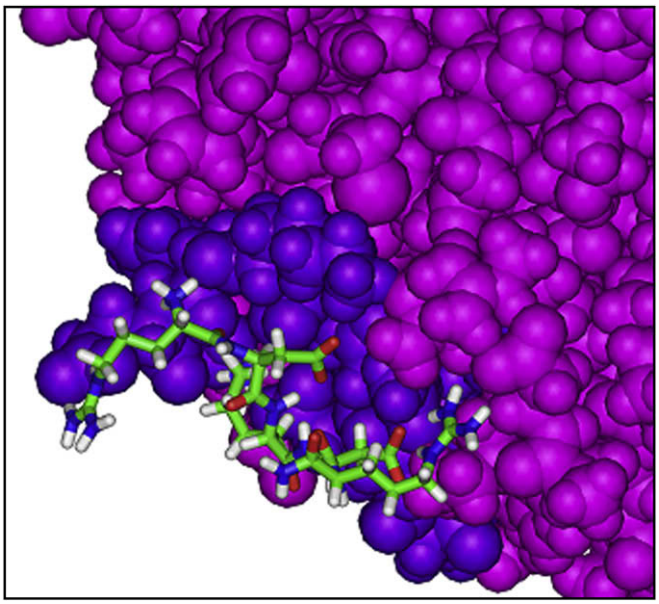

Fig. 5. Lowest energy conformation of the complex between H–ArgAspLysAspArg–NH_2 ligand (colored "by atom") and the γ (312–324) epitope (violet) comprised in the globular domain of the fibrin γ chain used for the simulation (magenta). (For interpretation of the references to colour in this figure legend, the reader is referred to the web version of this article.)

3. Results and discussion

3.1. SPR analysis

SPR experiments were carried out according to the protocol described in Section 2. The ligands under study were flowed onto fibrin-immobilized sensor chip at varying concentrations and data were fitted to the Langmuir model assuming a 1:1 binding interaction. For each compound the obtained sensorgrams were analyzed by means of the BIA evaluation 3.0.1 software.

The collected results are reported in Table 1. The reported K_D is obtained as a mean among experiments carried out at different values of flow rate (5 and 30 μl/min) and using different concentrations of the analytes (in the range of 0.01–1 mM). We could observe that four of the five peptides show K_D values between 17.5 and 34.4 μM while the H–ArgAspLysAspArg–NH_2 peptide is in the sub-micromolar range (250 nM). As an example we report one of the sensorgrams recorded at different concentrations (1, 0.5 and 0.1 mM) of the Ac–ArgAspLysAspArg–OH ligand. The black lines represent the lines fitted for each curve (Fig. 1).

3.2. MD simulations

MD simulations were performed on five fibrin–peptide complexes, a free fibrin sub-domain, and five free peptides to accurately estimate their binding free energies. To gauge whether the GB-MD simulations were stable and converged, energetic and structural properties were monitored during the course of all the trajectories as illustrated in Fig. 2 for H–ArgAspLysAspArg–NH_2 ligand with fibrin.

The monitored properties appear to properly converge before the data collection phase starting at 20 ps. Moreover, the stability of the systems was assessed by verifying that the difference between the average potential energy in the two halves of the considered trajectory was below 5 kcal/mol.

Structural properties were also monitored by computing the root–mean–square deviation (rmsd) between snapshots obtained during the course of the GB-MD trajectory and the original starting coordinates as illustrated in Fig. 3. Here, for H–ArgAspLysAspArg–NH_2 ligand in complex with fibrin, rmsd was computed for all heavy atoms, protein backbone main-chain atoms, and ligand heavy atoms.

In the fibrin/H–ArgAspLysAspArg–NH_2 peptide complex simulation, the fibrin structure appeared to be stable (rms deviation <1.5 Å), while the rms deviations of the H–ArgAspLysAspArg–NH_2 ligand structure (estimated within the complex) was observed to fluctuate in a larger amount. The fluctuations of the rms deviations in the ligand structure for the first 15 ps of simulation show that the

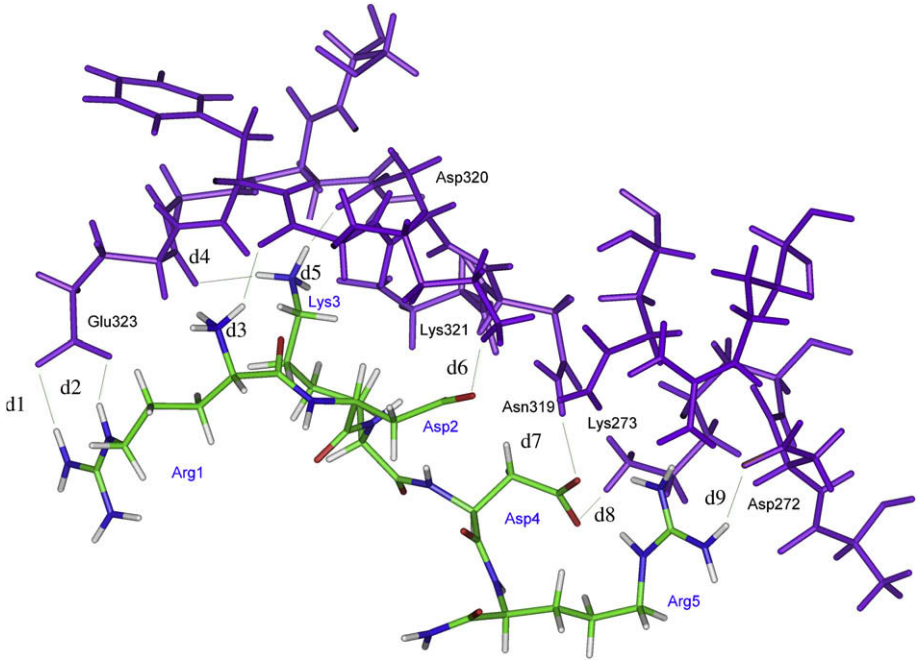

Fig. 6. Hydrogen bond network between the γ (312–324) epitope (comprised in the globular domain of the fibrin γ chain used for the simulation) and H–ArgAspLysAspArg–NH_2 ligand in the lowest energy conformation of the complex after MD sampling.

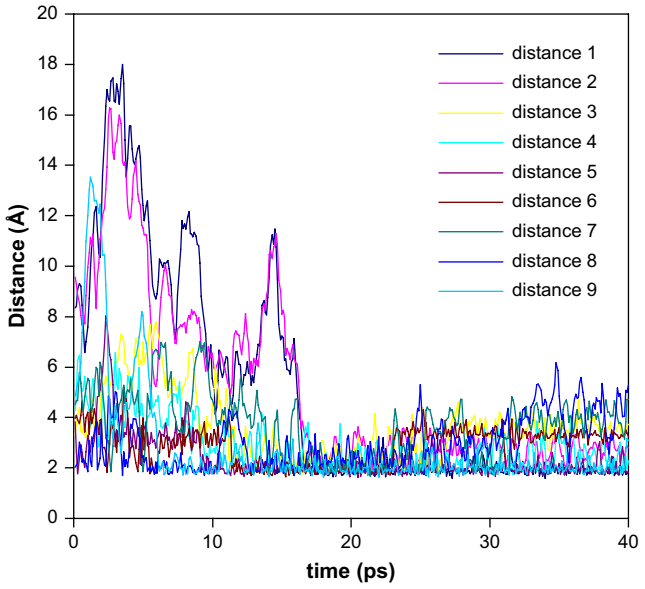

Fig. 7. Distance in Å of the selected hydrogen bonds versus time (ps) of the overall simulation (0–40 ps).

ligand initially underwent a major conformational change; only after that its structure was stable until the end of the simulation. That is reasonably due to the lower sampling power inherent to the molecular docking approach with respect to MD simulations.

3.3. Component analysis of binding free energies

The calculated and measured binding free energies (calculated as $\Delta G = -RT\ln K_D$) obtained for the group of peptides toward human fibrin are shown in Table 2.

The binding free energies calculated by MM-GBSA were in quite good agreement with our SPR data. The correlation coefficient between calculated and experimental binding free energies was 0.59, comparable to values already presented in the literature [18]. The correlation coefficients between the measured binding free energies and each component of the calculated figures were computed to identify which energetic factors were dominant for binding affinity (Table 2).

From the reported data one can envisage that nonpolar solvation contribution ($R^2 = 0.69$ for $\Delta G_{nonpolar}$) and, consequently, the difference in solvent-accessible solvation area ($R^2 = 0.64$ for ΔSASA,) give better correlation with binding affinity. The plot reported in Fig. 4 appears to suggest that the higher values of experimental ΔGs (obtained from the binding data) could also be fitted by lines with different slopes; nevertheless, a global agreement between experimental binding data and this component of the calculated binding energy is observed. The other components – the ΔE_{MM} ($R^2 = 0.09$), ΔG_{polar} ($R^2 = 0.03$), and the entropy contribution $T\Delta S$ ($R^2 = 0.005$) – do not show, instead, any significant correlation (Table 3). Therefore, the $\Delta G_{nonpolar}$ between the fibrin and the peptides can be considered to be the dominant factor for binding affinity (Fig. 4).

The most interesting aspect is that, in addition to $\Delta G_{nonpolar}$, the reduction of SASA upon binding, follows the same trend as the binding affinities of the individual ligands. In fact the ΔSASA is higher in the case of a ligand with higher binding affinity.

Table 4
Summary of the average distances between fibrin and H-ArgAspLysAspArg-NH_2 ligand of important hydrogen bonding interactions.

H-bond	Distance ID	Average distance[a]
Glu323@OE1···Arg1@HH21	Distance 1	2.16
Glu323@OE2···Arg1@HE	Distance 2	2.94
Lys321@O···Arg1@H3	Distance 3	3.09
Glu323@O···Lys3@HZ1	Distance 4	2.48
Asp320@OD1···Lys3@HZ2	Distance 5	2.00
Lys321@HZ2···Asp2@OD1	Distance 6	2.88
Asn319@HD21···Asp4@OD2	Distance 7	3.14
Lys273@HZ2···Asp4@OD1	Distance 8	3.20
Asp272@OD1···Arg5@HH12	Distance 9	2.02

[a] The distance are in Å[2].

Table 5
Occurrence of involvement of the fibrin residues in hydrogen bonds with the 5 ligands analyzed.

Residue	Occurrence	Residue	Occurrence
Asp 272[a]	20%	Asn 317	0%
Lys 273[a]	40%	Asp 318	80%
Gln 311[a]	40%	Asn 319	40%
Phe 312	0%	Asp 320	100%
Ser 313	0%	Lys 321	60%
Thr 314	0%	Phe 322	20%
Trp 315	0%	Glu 323	60%
Asp 316	0%	Gly 324	40%

[a] Residues external to the 312–324 interval.

3.4. Structural analysis

To highlight the features responsible for the binding between peptides and the globular domain of the γ chain of fibrin, the structural analysis was performed on the complex constituted by the selected domain of fibrin and the best performing peptide (H–ArgAspLysAspArg–NH_2) in its more stable conformation obtained after MD sampling (Fig. 5). It is possible to observe that in such complex a lot of hydrogen bonds (Fig. 6) stabilizing the interaction are formed between the epitope and the peptide.

By monitoring the hydrogen bonding interaction during all the simulation (Fig. 7) it was observed that most of the hydrogen bonds are retained during the trajectory and some other arose after the system reached the equilibrium (example, d1 and d2) thus meaning that they contribute to stabilizing the conformation of the peptide in the binding site. In Fig. 7, the distances in Å of these selected hydrogen bonds were reported versus time (ps) of the overall simulation (0–40 ps).

In Table 4 the average distances (in Å) of these hydrogen bonds during the 20–40 ps interval of the simulation are reported. It can be observed that these average distances vary from 2.00 to 3.20 Å meaning a good contribution to the stabilization of the complexes.

By analyzing the lowest energy conformation of the other complexes, a lower or equal number of hydrogen bonds can be observed between fibrin and each peptide with respect to the nine ones showed by fibrin/H–ArgAspLysAspArg–NH_2 complex (6 for H–LysGluArg–NH_2 and Ac–ArgAspLysAspArg–OH; 8 for H–LysGluLys–NH_2; 9 for H–LysAspArg–NH_2).

From the structural analysis of the investigated complexes emerges that some groups (Table 5) within the epitope are very important for the interaction with the ligands. In Table 5 the occurrence percentage for each residue of fibrin involved in hydrogen bonds with the ligands is reported (as number of complexes in which the hydrogen bond is present on five ligands). In particular it has been observed that the most important residues of the epitope involved in the interaction with the ligands appear to be Asp 318, Asp 320, Lys 312, Glu 323 with a occurrence percentage of 80, 100, 60 and 60, respectively.

4. Conclusions

Fibrin is an interesting target for the development of driving systems for the release of fibrinolytic drugs. In a previous work by

us, methods were proposed to design peptides, able to recognize the fibrin molecule, to be exposed on the surface of driving systems for targeted delivery of fibrinolytic drugs. It reports molecular modeling and docking calculations as well as preliminary SPR measurements. In the present paper new SPR studies were performed and an accurate computational approach was exploited to better understand the interactions between fibrin and its specific ligands.

It was found that the analyzed peptides could be considered interesting molecules showing K_D values ranging from 0.25 to 34.4 μM. The newly collected measurements do not significantly differ from the ones previously reported. The binding of the designed peptidic ligands to fibrin has been studied in quite more depth by means of the MM/GBSA method in combination with normal-mode analysis. Free energy calculation was carried out. By comparing experimental and calculated binding Δ*G*s (included single theoretical contributions) a good correlation was observed; in particular factors dominating the binding affinity were identified. The single contributions that were found to be in better agreement with the experimental Δ*G*s (as obtained from binding data) were the nonpolar solvation ones, and, consequently, the difference in solvent-accessible solvation areas.

The overall agreement between the calculated and experimental values for the ligands means that the MM/GBSA approach is a quite well suited tool for estimating protein–ligand interactions in the system of interest. From the structural analysis the major features responsible for the interaction between fibrin and ligands were drawn. In particular it has been observed that the most important residues of the epitope involved in the interaction with the ligands appear to be Asp 318, Asp 320, Lys 312, Glu 323. Moreover, the Asp 272, Lys 273, Gln 311 that are not comprised in the interval of interest, seem to play a significant role in enforcing the interaction of the ligands with the epitope. The importance of the Asp 318, Asp 320, Lys 321 and Glu 323 residues had already been highlighted in our previous design work [3], based on the DOCK screening (and relevant analysis of interactions).

The fluctuations observed at the beginning of the MD trajectory in the ligand structure, in comparison to the quite good stability of the target biomolecule, reasonably suggest that induced fit problems may not affect further molecular design studies, but the above observation also suggests that particular care needs to be put in the analysis of the active conformations of flexible ligands.

5. Experimental section

5.1. Samples

The ligand samples were prepared in house at Novetide. Fibrinogen from human plasma (F4883), and bovine thrombin (T4684) were purchased from Sigma. The ready-to-use HBS-EP from Biacore (0.01 M HEPES pH 7.4, 0.15 M NaCl, 3 mM EDTA, 0.005% Surfactant P20) was used as running buffer during the binding experiments. Reagents for amino coupling, *N*-hydroxysuccinimide (NHS), *N*-ethyl-*N*-dimethylaminopropyl)carbodiimide (EDC) and 1 M ethanolamine hydrocloride (pH 8.5), were supplied by Biacore as Amine Coupling Kit.

5.2. Interaction analysis

Biacore X system (Pharmacia, Inc.) was used to experimentally determine the kinetic constants of the fibrin–peptides interactions. The protocol is similar to the one described in a previous work [3]: only some of the involved analytes and a few operating parameters were changed during the new experiments in order to try to overcome some detection limit of the instrument and to get the target protein to retain at maximum its native conformation. Briefly, the sensor chip CM5 was preconditioned with a solution containing 1 M NaCl and 50 mM NaOH. A mixture of *N*-hydroxysuccinimide (NHS) and *N*-ethyl-*N*-(dimethylaminopropyl)-carbodiimide (EDC) was injected into the dextran matrix of the sensor chip to activate it at the flow rate of 5 μl/min at 37 °C. Human fibrinogen in 10 mmol/l sodium acetate (pH 4.6) was then immobilized on the matrix in an amount that give rise to a total signal of around 25,000 Ru. Since the baseline RU signal of the sensor chip is around 19,000, the ΔRU due to the fibrinogen immobilization is around 6000. The use of a quite high concentration of protein is allowed when high difference in molecular weight between analytes and protein does exist, as in this case. Furthermore, it must be considered that the initial amount of fibrinogen must be quite high because it will be submitted to the thrombin cleavage and a part of the signal will lose in this step.

During the immobilization, the matrix exceeding active sites were blocked with ethanolamine–HCl. A control surface for the contribution of the bulk refractive index was prepared using the same protocol, without fibrinogen injection, and directly deactivating the surface with ethanolamine after activation. All materials were dissolved in HBS-EP at pH 7.4, which was also used as running buffer. In order to convert immobilized fibrinogen into fibrin, 60 μl of 100 nmol/l thrombin were added at a flow rate of 2 μl/min. A marked decrease in the refractive index was recorded as a function of the time, while thrombin injection proceeded, so indicating loss of material, due to on-chip digestion.

In order to measure the association and dissociation constants between ligands and fibrin a continuous flow of HBS-EP running buffer was varied in a range of 5–30 μL/min, and different concentrations of ligands (0.01–1 mM) were injected through the immobilized fibrin. Different values of flow rates were used to check that no mass transfer phenomena exists. When the association and dissociation rate constants are approximately the same in different conditions of flow rate (as in this case) no mass transfer limitation has to be expected. The fibrin surface was regenerated after each binding interaction with 50 mM HCl at a flow rate of 5 μl/min for 60 s followed by re-equilibration with running buffer. The data were analyzed using the BIA evaluation 3.0 software to determine the association rate constant (k_{ass}) and the dissociation rate constant (k_{diss}) with a nonlinear least-squares method. K_D was obtained by calculating k_{diss}/k_{ass}.

Acknowledgments

This research was mostly supported by the EC-funded project G5RD-CT-2000-0294 (TATLYS) and by the Italian Ministry of Instructions University and Research (MIUR). The Authors also wish to thank the Dipartimento di Psichiatria, Neurobiologia, Farmacologia e Biotecnologie (DPNFB), University of Pisa, for the use of BIACORE facility, Prof. G. Giannaccini (DPNFB) for helpful suggestion in the use of BIACORE, the CINECA consortium for Amber7 facility, and Fondazione Salvatore Maugeri, Pavia (Italy) for scientific and financial support.

References

[1] K.G. Mann, in: W.N. Kelley (Ed.), Textbook of internal medicine, JB Lippincott Co., Philadelphia, 1992, pp. 1240–1245.
[2] J.W. Weisel, G.N. Phillips, C. Cohen, Nature 289 (1981) 263–267.
[3] A.M. Bianucci, I. Massarelli, F. Chiellini, C. Eidelman, E. Chiellini, J. Biomater. Sci. Polym. Ed. 15 (9) (2004) 1203–1222.
[4] W.J. Schielen, H.P. Adams, K. van Leuven, M. Voskuilen, G.I. Tesser, W. Nieuwenhuizen, Blood 77 (10) (1991) 2169–2173.
[5] T.A. Morton, D.G. Myszka, I.M. Chaiken, Anal. Biochem. 227 (1995) 176–185.
[6] I. Massova, P.A. Kollman, Perspect. Drug Discov. Des. 18 (2000) 113–135.
[7] I. Massova, P.A. Kollman, J. Am. Chem. Soc. 121 (1999) 8133–8143.
[8] B.R. Brooks, D. Janezic, M. Karplus, J. Comput. Chem. 16 (1995) 1522–1542.
[9] H.M. Berman, J. Westbrook, Z. Feng, G. Gilliland, T.N. Bhat, H. Weissig, I.N. Shindyalov, P.E. Bourne, Nucleic Acids Res. 28 (2000) 235–242.

[10] P.A. Kollman, I. Massova, C. Reyes, B. Kuhn, S. Huo, L. Chong, M. Lee, T. Lee, Y. Duan, W. Wang, O. Donini, P. Cieplak, J. Srinivasan, D.A. Case, T.E. Cheatham, Acc. Chem. Res. 33 (12) (2000) 889–897.
[11] G.D. Hawkins, C.J. Cramer, D.G. Truhlar, Chem. Phys. Lett. 246 (1995) 122–129.
[12] G.D. Hawkins, C.J. Cramer, D.G. Truhlar, J. Phys. Chem. 100 (1996) 19824–19839.
[13] AMBER Version 7; University of California at San Francisco: San Francisco, CA.
[14] H.J.C. Berendsen, J.P.M. Postma, W.F. Vangunsteren, A. Dinola, J.R. Haak, J. Chem. Phys. 81 (1984) 3684–3690.
[15] J.P. Ryckaert, G. Ciccotti, H.J.C. Berendsen, J. Comput. Phys. 23 (1977) 327–341.
[16] InsightII, Biosym/MSI, San Diego, CA, 1995.
[17] R.B. Rizzo, S. Toba, I.D. Kuntz, J. Med. Chem. 47 (12) (2004) 3065–3074.
[18] J. Wang, X. Kang, I.D. Kuntz, P.A. Kollman, J. Med. Chem. 48 (2005) 2432–2444.